Al-Mustansiriyah Journal of Science
ISSN: 1814-635X (print), ISSN:2521-3520 (online) Volume 33, Issue 4, 2022 DOI: http://doi.org/10.23851/mjs.v33i4.1216

Research Article **Open Access**

Influence of Graphene Sheets Accumulation on Optical Band Gap Enhanced Graphite Exfoliation

Riad M. Hameed, Ahmed Al-Haddad*, Abbas K. H. Albarazanchi

Department of Physics, College of Science, Mustansiriyah University, Baghdad, IRAQ.

*Correspondent contact: ahmed.al-haddad@uomustansiriyah.edu.iq

Article Info

Received
29/08/2022

Accepted
02/10/2022

Published
30/12/2022

ABSTRACT

Recently, graphene has been adopted to replace other expansive materials in various devices that perform numerous functionalities in many industrial fields. Meanwhile, researchers are still investigating the amazing properties of graphene. Herein, reduced graphene oxide (rGO) has been successfully exfoliated directly using a graphite rod in a modified electrolyte including a table salt as a co-electrolyte. The structure of graphene obtained by using exfoliation methods shows a low ratio of O/C and confirms the high crystallinity of rGO. The thickness of rGO was adjusted during the drying of the drops of rGO solution and obtained about an 8-80 nm rGO thick. The increased O/C ratio and crystallinity enhancement could be attributed to the quantum confinement effect. Further investigations to estimate the decay constant of the optical band gap during the thinning of the rGO layers show that the optical band gap was associated with thicknesses of the rGO at a decay constant of 0.3367±0.00205. These results would be crucial in several optical applications that depend on the thicknesses and the band gap.

KEYWORDS: 2-D materials; graphene; rGO; exfoliation; energy gap shifting.

INTRODUCTION

Since the achievement of single graphene sheets by Novoselov and Geim in 2004 [1], graphene grows much attention because of its unique properties such as (the 2-D crystal structure thinnest reachable crystal, good thermal conductivity, and high electron mobility. Therefore, graphene has been used in a wide range of applications including energy storage [2, 3], thermal management [4, 5], armorer [6], optoelectronic [7], biosensor materials [8], etc. Meanwhile, the preparation of graphene with a low O/C ratio via a low-cost and uncomplicated technique is an important feature of industrial evolution.

Recently, a promising technique named graphite exfoliation has the potential to address the large-scale production of graphene [9-11]. This technique can create a monolayer of graphene from graphite with several oxygen functional groups resulting in graphene oxide (GO) [12, 13]. The presence of these oxygen-containing functional groups increases hydrogen bonding with water and other organic molecules, resulting in hydrophilic characteristics, and making other graphene-based materials easier to modify [14, 15]. The oxidation reaction is thought to be responsible for the creation of sp^3 domains in GO [14-16]. This enhancement in GO characteristics could be useful in graphene-based application research. The structures of graphite oxide and GO are similar, and both have layered configurations with oxygen functional groups on the basal plane and edge [17]. For their reliable visible light absorption, reduced GO (rGO) is distinguished as the intensive material that was studied recently [18, 19]. To tune the optical absorption of rGO various methodologies are obtained such as quantization of the structure [20], doped with metal [21], binary and trinary composites [22, 23], and heterostructure [24, 25].

To evolute GO and reduced the oxygen to a lower degree, the exfoliation approach often performs better than the cathodic method (single- to few-layered nanosheets). Herein, the achievement of a low-priced and remarkably simple molecule NaCl could work as a co-electrolyte to prevent oxidation during the exfoliation of graphite. In addition, the ability to produce graphene with the lowest amount

of oxidation and high structural quality. Furthermore, optical absorption enhancement can be obtained by increasing the layers of the rGO. This improvement of the optical absorption by an accumulation of rGO nanolayers could optimize many applications and devices such as solar energy conversion, photocatalyst, LED, and photodetectors.

MATERIALS AND METHODS

To exfoliate a high purity graphite rod with a radius of 6.5mm, a positive voltage (10 V) was applied to the graphite rod as a working electrode with platinum foil as a counter electrode. The procedure was carried out in an aqueous solution with 0.1 M Na_2SO_4 as the primary (exfoliating) electrolyte and a specific molar concentration of different chemicals as the potential oxidation-preventing agent (for example, 0.3 M NaCl). 20 mm height of graphite rod was in the electrolyte to equalize the surface area between the working and counter electrodes. Both electrodes were immersed in an 80 mL aqueous electrolyte solution that contained 0.1 M Na_2SO_4 as the primary electrolyte. NaCl provided the greatest results in terms of avoiding oxidation of the exfoliated graphene nanosheets. Using a PeakTech 6227 DC power supply, a positive voltage of 10V was delivered to the graphite foil electrode for 1 hour to delaminate the graphite. At the same time, the platinum counter electrode was maintained parallel to the graphite foil surface at a distance of around 2 cm. The graphite electrode outer layers were seen to swell and expand during the electrolytic process, producing numerous millimeter-sized fragments that broke off from the electrode and tended to float on the aqueous solution. These pieces were then collected, rinsed with water, and then filtered (5 μm filter paper), the fine resulting graphene was left to dry for over 12 hours at room temperature. The swelling graphitic material that had not yet separated from the electrode was also removed in this process. To obtain a colloidal suspension (supernatant) of graphene layers, the resulting product was transferred to a water/isopropanol mixture (65/35 v/v % percent) and sonicated in an ultrasound bath cleaner for 20 min.

The TESCAN MIRA 3 scanning electron microscope (SEM) was used to analyze the resulting graphene morphology. The crystal structural investigation of the rGO layers was carried out through X-ray diffraction (LabX XRD-6000 Shimadzu) at room temperature. The range of 2θ was fixed from 5° to 70° for all samples. rGO solution (0.2g rGO+100 ml DI water) was dropped on a glass slide as a substrate (each drop is 0.5 ml of rGO solution), then dried at 60°C, the samples were characterized with a T70/T80 Series UV-Vis-Near IR spectrometer. The scan range was set from 200 to 800 nm. Figure 1 illustrates the schematic of the preparation procedures starting from step (1) exfoliation of graphite rod, step (2) dried rGO, step (3) diluted rGO with DI water, step (4) dried drop number of rGO solution accumulation on the glass substrates, and step (5) the samples for optical analytic, it can be noted that the samples are not optically homogeneous, however, the centers of the samples are partially homogeneous and all measurements account this fact.

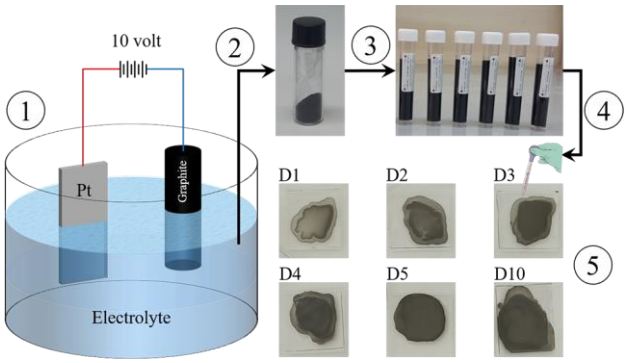

Figure 1. Schematic diagram of the electrochemical graphite exfoliation and sample preparation of rGO, D1-D10 refers to drops number (layer number).

RESULTS AND DISCUSSION

SEM image in Figure 2a confirms the presence of the rGO nanosheets realized from 10 drops of rGO solution on the glass substrate. Figure 2b illustrates the SEM of a single nanosheet of rGO obtained from one drop of rGO solution, the nanosheet has a thickness of around 8 nm (for 0.5 ml of dried rGO solution) which can be noted also from the EDX line-scan profile of the selective area in Figure 2c. Moreover, Figure 2c reveals a high C and low O atoms, accordingly, the O/C ratio is extremely low (0.0356 on average).

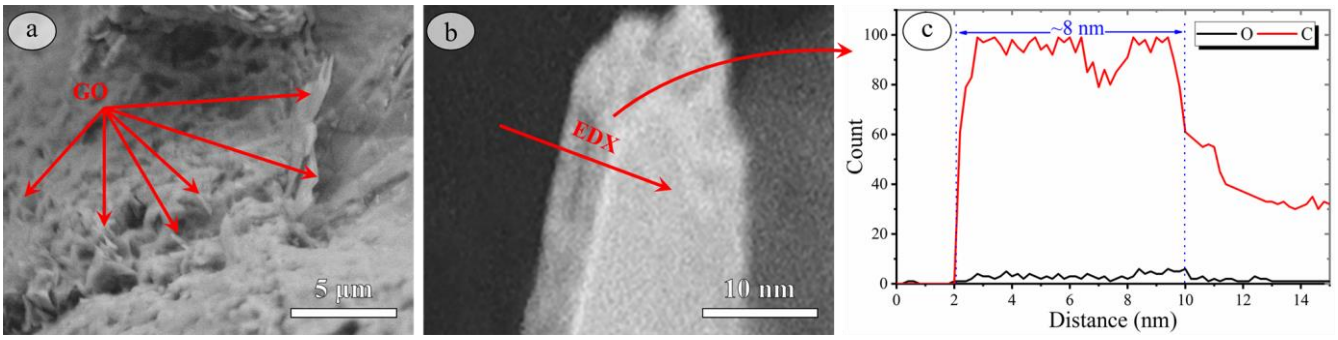

Figure 2. a) SEM image of the prepared rGO, b) a magnified SEM of a single layer of rGO, c) EDX line-scan profile of the red arrow in the magnified SEM.

XRD investigation of the pattern of graphite, GO (exfoliation without adding NaCl), and rGO describes the crystal structures of the materials that were used and prepared in this study which are illustrated in Figure 3.

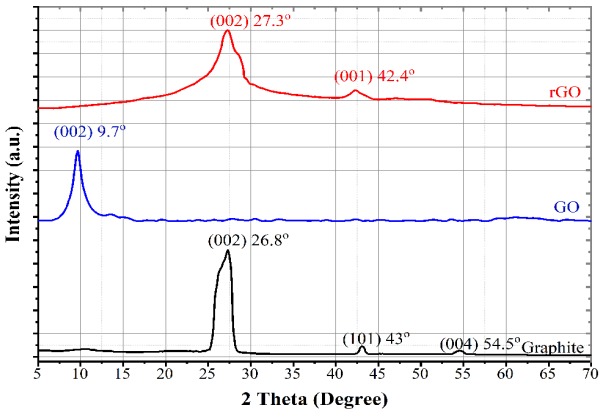

Figure 3. XRD patterns of the graphite and the prepared GO and rGO samples.

The peaks indexed at 2θ = 26.8°, 2θ = 43°, and 2θ = 54.5° signify the crystalline structure of graphite with reflection (002), (101), and (004), respectively [26, 27]. It can be distinguished that the dominant peak (002) of graphite at 2θ = 26.8° corresponds to d = 3.3 Å. XRD patterns of GO are also gauged and it has only one dominant peak, GO exhibits a narrow peak (002) at 2θ = 9.6° corresponding to d = 9.13 Å. The d-spacing in GO has increased from that of a crystalline graphite sample upon oxidation. The depicted rGO XRD pattern presents almost broad two peaks (002), (001) at positions 27.3°, 42.3°, the calculated d-spacings are 3.3, 2.1 Å, and crystallite sizes are 2.592, 5.318 nm, respectively. Consequently, the XRD data of the prepared samples are proof of concept, whereas the presence of only one XRD peak of GO suggests complete oxidation of graphite with high crystallinity of the GO [16, 28]. Moreover, XRD peaks of rGO support the presence of an Oxygen minority [29]. In addition, the high crystallinity of GO and rGO is compatible with previous literature [30, 31] The d-spacings, crystallite sizes, and peaks planes were calculated according to Bragg's law of diffraction, Debye Scherrer's formula, and Match! software for phase analysis, respectively [32-34].

Figure 4 demonstrates all the rGO samples with different accumulative layer thicknesses (8, 16, 24, 32, 40, and 80 nm) correspond to dried drop numbers of rGO solution (D1, D2, D3, D4, D5, and D10), respectively. The samples have the highest absorption at UV spectra due to the aromatic C-C bonds which is consistent with other reports [35-37]. Interestingly, the UV absorbance of rGO is significant thickness-dependent in the wavelength range of 270-455 nm. The absorbance of the samples D1, D2, D3, D4, D5, and D10 produce a shift towards a higher wavelength (visible spectra) respectively, which is reasonable because the samples became darker with increasing the thickness of the rGO layer as shown in Figure 1 step (5).

It is known that the Lambert-Beer law is the principle of UV absorption-based quantification, where the concentration of the samples is directly proportional to their absorbance at a given wavelength [37]. In addition, the rGO samples have absorbance at 270 nm, which originates from the $\pi \rightarrow \pi^*$ transitions of aromatic C=C bonds within rGO sheets. The inset shows the relationship between the rGO thickness and the absorbance maximum. It complies quite well with the Beer-Lambert law. The absorption peak of rGO gradually moves during the chemical reduction process from 270 nm to 455 nm, and the absorption in the entire spectral region rises. these observations suggest the gradual restoration of the $\pi \rightarrow \pi$ conjugated structure within the graphene nanosheets [38].

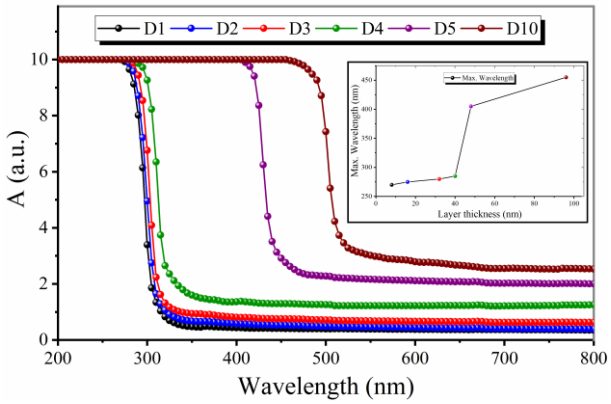

Figure 4. Absorbance spectra of the prepared rGO samples in step (5) from the Figure. 1, the inset figure is the calculated maximum wavelength as a function of rGO thicknesses.

Whereas graphene has been classified as a typical indirect semiconductor and based on the absorbance spectra of the rGO sample, an indirect transition model was utilized to evaluate the optical band gap (E_g) values of each prepared thickness (layers) [39, 40], as shown in Figure 5.

$$\alpha = \left(h\gamma - E_g\right)^2 / h\gamma \quad (1)$$

where α is the absorption coefficient, h is Planck's constant, and γ is the frequency.

Through the calibration of the E_g values from experiment absorbance spectra, it was noted that the increase of rGO thickness was associated with the optical indirect band gap narrowing.

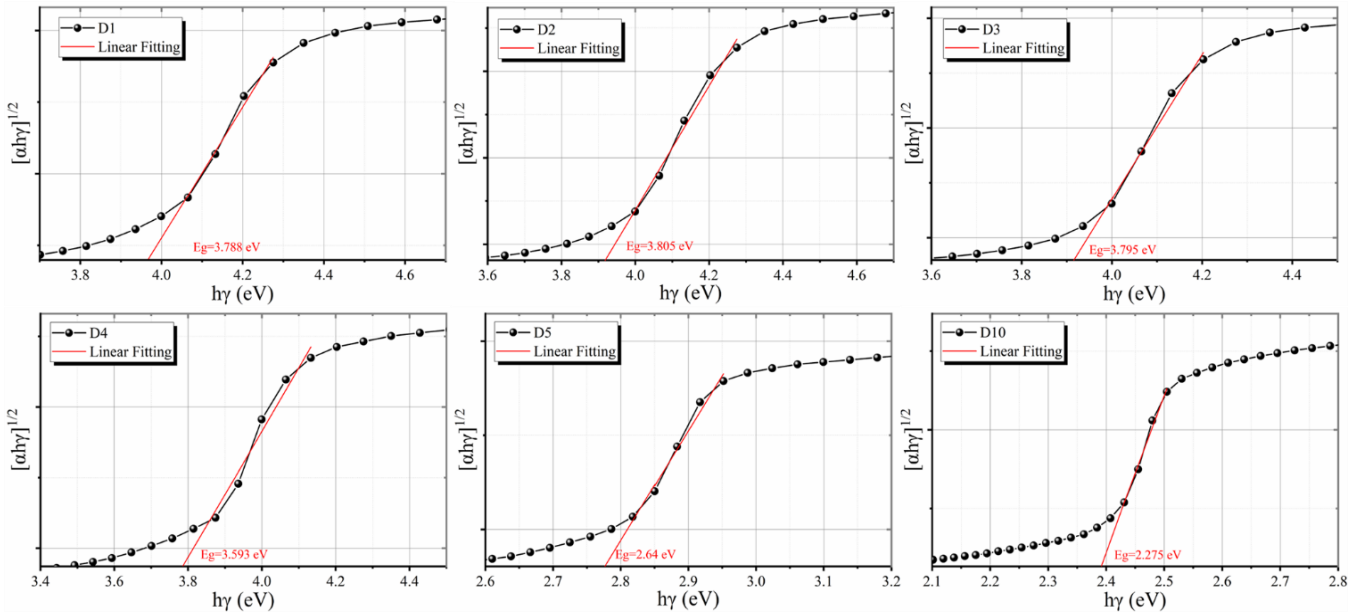

Figure 5. Tauc plot for optical band gap determination for rGO samples (D1, D2, D3, D4, D5, and D10), respectively.

Moreover, the directly proportional relationship of thickness with E_g values (i.e., plots of E_g versus layers) can be presented in another aspect as shown in Figure 6. To find a general analysis, the curve in Figure 6 fitted with the increase the thickness and decreasing the E_g presenting a decay feature that could be construed by a single-exponential model using the equation:

$$E_g = Ae^{-\omega/\tau} \quad (2)$$

where A is a constant and ω is the thickness of rGO, τ is the decay constant.

The resulting decay constant is secured at 0.3367±0.00205.

This result confirms the quantum confinement effect that occurs if one of the dimensions is less than their exciton Bohr radius (for graphene it depends on the O/C ratio) [33-36]. Generally, the quantum confinement effect is clearly observed in our samples which relates to a low value of the O/C ratio (0.0356 on average) and the exciton Bohr radius is higher when the O/C ratio becomes lower [35]. Therefore, it can be concluded that the redshift can be observed by increasing the rGO layers.

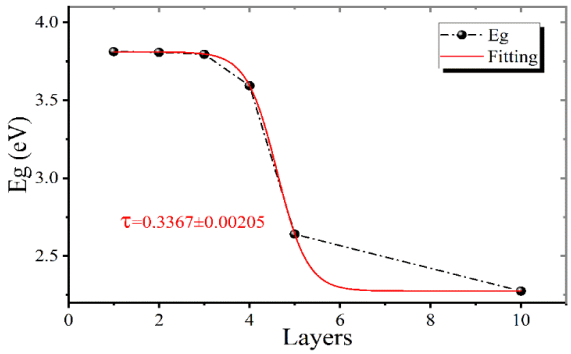

Figure 6. Band gap energy as a function of rGO nanosheet thickness. The red fitting curve presents a decay constant as 0.3367±0.00205.

CONCLUSIONS

We have investigated the structure of the graphene obtained via exfoliation methods by adding 0.3 M of NaCl as a co-electrolyte to prevent oxidation during the exfoliation of graphite. EDX results exhibited a low ratio of O/C (0.0356). The XRD patterns of the prepared samples ensure existing of the high crystallinity of GO and rGO. By tuning the rGO accumulation layered thicknesses, the resulting absorption band exposed a redshift caused by the quantum confinement effect that could be related to increasing the O/C ratio and crystallinity enhancement. The estimated decay constant of the optical band gap over the rGO layers demonstrated that the accuracy of the optical band gap was associated with the thicknesses of the rGO. Thus, this paper provides new data for the enhancement of the light absorbance of rGO with a low ratio of O/C that could improve many optical applications.

ACKNOWLEDGMENT

The authors would like to acknowledge RES laboratory, department of physics, college of sciences, Mustansiriyah University, Baghdad, Iraq. Furthermore, the authors distinguish the effort of Nanostructures and Applied Spectroscopy Research Group for their collaboration and using their scientific facilities.

Disclosure and conflict of interest: The authors declare that they have no conflicts of interest.

REFERENCES

[1] K. S. Novoselov et al., "Electric field effect in atomically thin carbon films," Science, vol. 306, no. 5696, pp. 666-669, 2004. https://doi.org/10.1126/science.1102896

[2] R. Vellacheri, A. Al-Haddad, H. Zhao, W. Wang, C. Wang, and Y. Lei, "High performance supercapacitor for efficient energy storage under extreme environmental temperatures," Nano Energy, vol. 8, pp. 231-237, 2014. https://doi.org/10.1016/j.nanoen.2014.06.015

[3] S. Wang, B. Yang, H. Chen, and E. Ruckenstein, "Reconfiguring graphene for high-performance metal-ion battery anodes," Energy Storage Materials, vol. 16, pp. 619-624, 2019. https://doi.org/10.1016/j.ensm.2018.07.013

[4] G. Xin et al., "Large-area freestanding graphene paper for superior thermal management," Advanced Materials, vol. 26, no. 26, pp. 4521-4526, 2014. https://doi.org/10.1002/adma.201400951

[5] F. Kargar, Z. Barani, M. Balinskiy, A. S. Magana, J. S. Lewis, and A. A. Balandin, "Dual-functional graphene composites for electromagnetic shielding and thermal management," Advanced Electronic Materials, vol. 5, no. 1, p. 1800558, 2019. https://doi.org/10.1002/aelm.201800558

[6] N. Dey et al., "Graphene materials: Armor against nosocomial infections and biofilm formation-A review," Environmental Research, p. 113867, 2022. https://doi.org/10.1016/j.envres.2022.113867

[7] C. Xie, Y. Wang, Z.-X. Zhang, D. Wang, and L.-B. Luo, "Graphene/semiconductor hybrid heterostructures for optoelectronic device applications," Nano Today, vol. 19, pp. 41-83, 2018. https://doi.org/10.1016/j.nantod.2018.02.009

[8] G. Yildiz, M. Bolton-Warberg, and F. Awaja, "Graphene and graphene oxide for bio-sensing: General properties and the effects of graphene ripples," Acta Biomaterialia, vol. 131, pp. 62-79, 2021. https://doi.org/10.1016/j.actbio.2021.06.047

[9] A. C. Ferrari et al., "Science and technology roadmap for graphene, related two-dimensional crystals, and hybrid systems," Nanoscale, vol. 7, no. 11, pp. 4598-4810, 2015.

[10] A. Abdelkader, A. Cooper, R. A. Dryfe, and I. Kinloch, "How to get between the sheets: a review of recent works on the electrochemical exfoliation of graphene materials from bulk graphite," Nanoscale, vol. 7, no. 16, pp. 6944-6956, 2015. https://doi.org/10.1039/C4NR06942K

[11] S. Yang, M. R. Lohe, K. Müllen, and X. Feng, "New-generation graphene from electrochemical approaches: production and applications," Advanced Materials, vol. 28, no. 29, pp. 6213-6221, 2016. https://doi.org/10.1002/adma.201505326

[12] J. Guerrero-Contreras and F. Caballero-Briones, "Graphene oxide powders with different oxidation degree, prepared by synthesis variations of the Hummers method," Materials Chemistry and Physics, vol. 153, pp. 209-220, 2015. https://doi.org/10.1016/j.matchemphys.2015.01.005

[13] D. A. Dikin et al., "Preparation and characterization of graphene oxide paper," Nature, vol. 448, no. 7152, pp. 457-460, 2007. https://doi.org/10.1038/nature06016

[14] M. Veerapandian, Y.-T. Seo, H. Shin, K. Yun, and M.-H. Lee, "Functionalized graphene oxide for clinical glucose biosensing in urine and serum samples," International Journal of Nanomedicine, vol. 7, p. 6123, 2012. https://doi.org/10.2147/IJN.S38402

[15] V. Panwar, A. Chattree, and K. Pal, "A new facile route for synthesizing of graphene oxide using mixture of sulfuric-nitric-phosphoric acids as intercalating agent," Physica E, vol. 73, pp. 235-241, 2015. https://doi.org/10.1016/j.physe.2015.06.006

[16] K. P. Loh, Q. Bao, G. Eda, and M. Chhowalla, "Graphene oxide as a chemically tunable platform for optical applications," Nature Chemistry, vol. 2, no. 12, pp. 1015-1024, 2010. https://doi.org/10.1038/nchem.907

[17] S. Y. Toh, K. S. Loh, S. K. Kamarudin, and W. R. W. Daud, "Graphene production via electrochemical reduction of graphene oxide: Synthesis and characterisation," Chemical Engineering Journal, vol. 251, pp. 422-434, 2014. https://doi.org/10.1016/j.cej.2014.04.004

[18] S. K. Abdel-Aal and A. S. Abdel-Rahman, "Graphene influence on the structure, magnetic, and optical properties of rare-earth perovskite," Journal of Nanoparticle Research, vol. 22, no. 9, pp. 1-10, 2020. https://doi.org/10.1007/s11051-020-05001-7

[19] V. Kumar, "Linear and nonlinear optical properties of graphene: a review," Journal of Electronic Materials, vol. 50, no. 7, pp. 3773-3799, 2021. https://doi.org/10.1007/s11664-021-08904-w

[20] X. Hai, J. Feng, X. Chen, and J. Wang, "Tuning the optical properties of graphene quantum dots for biosensing and bioimaging," Journal of Materials Chemistry B, vol. 6, no. 20, pp. 3219-3234, 2018. https://doi.org/10.1039/C8TB00428E

[21] G. Wang et al., "Facile and highly effective synthesis of controllable lattice sulfur-doped graphene quantum dots via hydrothermal treatment of durian," ACS Applied Materials & Interfaces, vol. 10, no. 6, pp. 5750-5759, 2018. https://doi.org/10.1021/acsami.7b16002

[22] F. Usman et al., "Synthesis and characterisation of a ternary composite of polyaniline, reduced graphene-oxide and chitosan with reduced optical band gap and stable aqueous dispersibility," Results in Physics, vol. 15, p. 102690, 2019. https://doi.org/10.1016/j.rinp.2019.102690

[23] Y. Jin, Y. Zheng, S. G. Podkolzin, and W. Lee, "Band gap of reduced graphene oxide tuned by controlling functional groups," Journal of Materials Chemistry C, vol. 8, no. 14, pp. 4885-4894, 2020. https://doi.org/10.1039/C9TC07063J

[24] B. Qiu, X. Zhao, G. Hu, W. Yue, X. Yuan, and J. Ren, "Tuning optical properties of Graphene/WSe2 heterostructure by introducing vacancy: First principles calculations," Physica E, vol. 116, p. 113729, 2020. https://doi.org/10.1016/j.physe.2019.113729

[25] A. Bafekry, M. Obeid, C. V. Nguyen, M. Ghergherehchi, and M. B. Tagani, "Graphene hetero-multilayer on layered platinum mineral jacutingaite (Pt 2 HgSe 3): van der Waals heterostructures with novel optoelectronic and thermoelectric performances," Journal of Materials Chemistry A, vol. 8, no. 26, pp. 13248-13260, 2020. https://doi.org/10.1039/D0TA02847A

[26] B. Zhao et al., "A highly thermally conductive electrode for lithium ion batteries," Journal of Materials Chemistry A, vol. 4, no. 38, pp. 14595-14604, 2016. https://doi.org/10.1039/C6TA04774B

[27] A. Ramesh, M. Jeyavelan, and M. S. L. Hudson, "Electrochemical properties of reduced graphene oxide derived through camphor assisted combustion of graphite oxide," Dalton Transactions, vol. 47, no. 15, pp. 5406-5414, 2018. https://doi.org/10.1039/C8DT00626A

[28] S. Thakur and N. Karak, "Green reduction of graphene oxide by aqueous phytoextracts," Carbon, vol. 50, no. 14, pp. 5331-5339, 2012. https://doi.org/10.1016/j.carbon.2012.07.023

[29] H. Maharana, P. K. Rai, and A. Basu, "Surface-mechanical and electrical properties of pulse electrodeposited Cu-graphene oxide composite coating for electrical contacts," Journal of Materials Science, vol. 52, no. 2, pp. 1089-1105, 2017. https://doi.org/10.1007/s10853-016-0405-7

[30] J. Munuera, J. Paredes, S. Villar-Rodil, A. Castro-Muñiz, A. Martínez-Alonso, and J. Tascón, "High quality, low-oxidized graphene via anodic exfoliation with table salt as an efficient oxidation-preventing co-electrolyte for water/oil remediation and capacitive energy storage applications," Applied Materials Today, vol. 11, pp. 246-254, 2018. https://doi.org/10.1016/j.apmt.2018.03.002

[31] F. Liu et al., "Synthesis of graphene materials by electrochemical exfoliation: Recent progress and future potential," Carbon Energy, vol. 1, no. 2, pp. 173-199, 2019. https://doi.org/10.1002/cey2.14

[32] A. Richel, N. Johnson, and D. McComb, "Observation of Bragg reflection in photonic crystals synthesized from air spheres in a titania matrix," Applied Physics Letters, vol. 76, no. 14, pp. 1816-1818, 2000. https://doi.org/10.1063/1.126175

[33] P. Scherrer, "Bestimmung der große und der inneren struktur von kolloidteilchen mittels rontgenstrahlen," vol. Klasse, 2, ed: Nachrichten von der Gesellschaft der Wissenschaften zu Gottingen, 1918.

[34] A. Patterso, "The Scherrer formula for I-ray particle size determination," J. Phys. Rev, vol. 56, no. 10, pp. 978-982, 1939. https://doi.org/10.1103/PhysRev.56.978

[35] R. Y. Gengler et al., "Revealing the ultrafast process behind the photoreduction of graphene oxide," Nature Communications, vol. 4, no. 1, pp. 1-5, 2013. https://doi.org/10.1038/ncomms3560

[36] P. Bolibok, K. Roszek, and M. Wiśniewski, "Graphene oxide-mediated protection from Photodamage," The Journal of Physical Chemistry Letters, vol. 9, no. 12, pp. 3241-3244, 2018. https://doi.org/10.1021/acs.jpclett.8b01349

[37] Ł. Tymecki, M. Pokrzywnicka, and R. Koncki, "Paired emitter detector diode (PEDD)-based photometry-an alternative approach," Analyst, vol. 133, no. 11, pp. 1501-1504, 2008. https://doi.org/10.1039/b807127f

[38] D. Li, M. B. Müller, S. Gilje, R. B. Kaner, and G. G. Wallace, "Processable aqueous dispersions of graphene

nanosheets," Nature Nanotechnology, vol. 3, no. 2, pp. 101-105, 2008. https://doi.org/10.1038/nnano.2007.451

[39] M. Velasco-Soto, S. Pérez-García, J. Alvarez-Quintana, Y. Cao, L. Nyborg, and L. Licea-Jiménez, "Selective band gap manipulation of graphene oxide by its reduction with mild reagents," Carbon, vol. 93, pp. 967-973, 2015. https://doi.org/10.1016/j.carbon.2015.06.013

[40] A. K. Albarazanchi, A. Al-Haddad, and M. F. Sultan, "Plasmonic Enhancement Mechanism of Template-Based Synthesized Au@TiO2 Nanodiscs," ChemNanoMat, vol. 7, no. 1, pp. 27-33, 2021. https://doi.org/10.1002/cnma.202000513

How to Cite

R. M. Hameed, A. Al-Haddad, and A. K. H. . Albarazanchi, “Influence of Graphene Sheets Accumulation on Optical Band Gap Enhanced Graphite Exfoliation”, *Al-Mustansiriyah Journal of Science*, vol. 33, no. 4, pp. 168–174, Dec. 2022.